

Tertiary amines from RCF lignin mono- and dimers: Catalytic N-functionalized antioxidants from wood

Dieter Ruijten[†], Thomas Narmon[†], Korneel Van Aelst[†], Hanne De Weert[†], Robbe van der Zweep[†], Tessy Hendrickx[†], Claude Poleunis[‡], Lingfeng Li[§], Kevin M. Van Geem[§], Damien P. Debecker[‡], Bert F. Sels^{†}*

[†] Centre for Sustainable Catalysis and Engineering, KU Leuven, Celestijnenlaan 200F, 3001 Leuven, Belgium. (Corresponding author email: bert.sels@kuleuven.be)

[‡] Institute of Condensed Matter and Nanosciences (IMCN), Université Catholique de Louvain (UCLouvain), 1348 Louvain-La-Neuve, Belgium

[§] Laboratory for Chemical Technology, Ghent University, Technologiepark 121, 9052 Ghent, Belgium

KEYWORDS: Bio-based amines, Lignin upgrading, hydrogen borrowing, Antioxidant, Heterogeneous catalysis

ABSTRACT

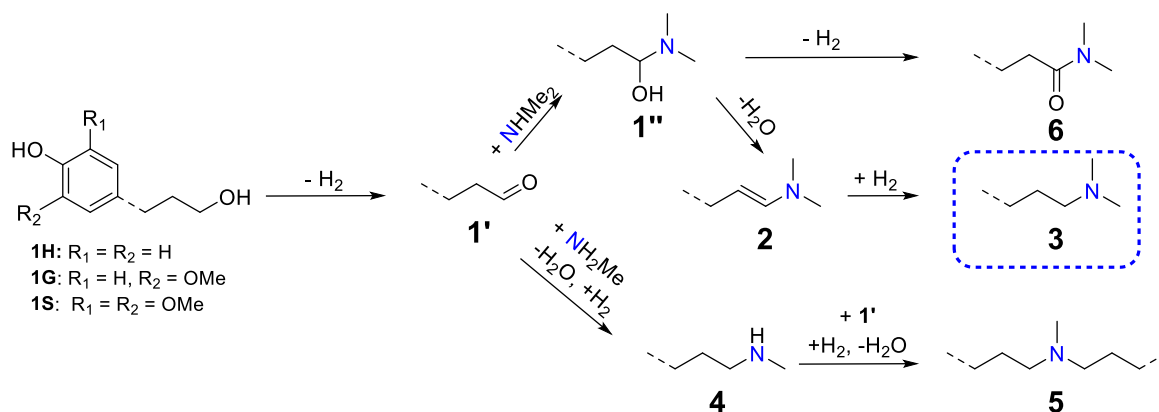
Functionalization of bio-based aromatics offers an appealing opportunity towards a renewable way of fulfilling our current needs for chemicals and materials. Here, an atom efficient Cu-catalyzed hydrogen borrowing strategy is presented, which successfully functionalizes

aliphatic alcohols in aromatic monomers and dimers, derived from lignin by reductive catalytic fraction (RCF), into tertiary dimethylamines. Kinetic experiments and ToF SIMS analysis of the supported copper catalyst demonstrated a reduced catalytic activity for monomeric methoxyphenolics, such as guaiacol and syringols, relative to phenolic and nonphenolic model compounds. This is explained by the formation through demethylation, and adsorption of strong coordinating catechol species. The nature of the catalyst support proved to be key to cope with the catechol deactivation and keep high catalytic activity, with Cu supported on SiO₂ outperforming earlier reported Cu-ZrO₂. The hydrogen borrowing method was extended to real spruce wood-derived RCF lignin oil fractions, containing both phenolic mono- and oligomers. Special effort was done to identify the composition and molecular structure of the resulting phenolic dimer amines by GC x GC – TOF/MS and ¹H-¹³C-NMR techniques. The stable lignin-derived tertiary amines displayed excellent antioxidant activity during an ABTS assay, highlighting the added value of the products obtained by the hydrogen borrowing upgrading strategy.

INTRODUCTION

Tertiary amines are prevalent structural moieties in agrochemicals, medicines and polymer materials.^{1–4} Various methods exist for their synthesis, mainly starting from petro-based precursors^{5–8}, with more sustainable pathways starting from bio-based precursors being highly sought-after.^{9,10} In this context, amination of lignin-derived phenolics, having aliphatic alcohol groups, is an elegant strategy to create phenolics featuring an alkyl tertiary amine group. In order to transform alcohols into amines, hydrogen borrowing (HB) has proven itself as an (atom-)efficient and straightforward methodology.^{11–14} Lignin-derived monomers dihydroconiferyl alcohol (**1G**) and dihydrosinapyl alcohol (**1S**) have successfully been aminated with NH₃¹⁵ and various secondary amines^{16,17} using both homogeneous (Ru) and heterogeneous (Ni, Cu) catalysts following this HB strategy. The mechanism involves initial

alcohol dehydrogenation to a carbonyl intermediate, subsequent *in situ* condensation with the amine reactant and final hydrogenation to the amine product, as illustrated in Scheme 1 for dimethylamine (DMA). When a secondary amine reactant is applied, the formation of the amide and secondary amine (by reactant disproportionation) products are important side reactions. By adequately selecting the reaction parameter, their formation can be limited effectively, with hydrogen pressure and catalyst selection being most essential.¹⁶ Despite good yields, catalytic amination of lignin-derived guaiacols and syringols, containing aliphatic alcohols requires relative harsh conditions (i.e., high temperature, high catalyst loading, long reaction time) compared to similar amination of less complex aliphatic alcohols.¹⁸ Preferential coordination of the phenolic group to the catalyst surface and catalyst deactivation have been proposed as possible causes, but dedicated studies on this issue are still lacking in literature.^{15,19}



Scheme 1. Proposed Hydrogen Borrowing amination (HB) pathway for the coupling of RCF lignin monomers with DMA towards tertiary amine **3**, using a supported Cu catalyst.

A recent game changer in lignocellulose biorefining to access chemicals from lignin, is Reductive Catalytic Fractionation (RCF). This technology enables high lignocellulose biomass delignification, and simultaneously yields a low molar mass (< 1000 Da) depolymerised lignin product with high phenolic OH (up to 4 mmol OH g⁻¹) and tunable aliphatic OH functionality (1-5 mmol g⁻¹).²⁰ RCF thus holds high promise to obtain soluble and reactive lignin products,

ideal for further functionalization.^{21,22} The obtained refined lignin oil (RFLO) is a complex mixture of both monomeric and oligomeric phenolics. The soluble sugars are removed in the RFLO by a washing step with water. The molecular structure of RCF derived products is fairly known, in contrast to that of other (technical) lignin products, such as Kraft. Only recently, our group managed to identify more than 80% of the molecular structures using ¹H–¹³C HSQC NMR and GC x GC-FID/MS, as opposed to 45% for Kraft.^{23–25} Previous work on the amination of lignin-derived phenolics focused exclusively on the phenolic monomeric compounds. However, having this recent detailed molecular insight of the RCF lignin oil opens the possibility for the amination of the dimeric and oligomeric phenolics fraction with elaborate molecular understanding.

Due to the abundant phenolic moieties in RCF lignin-derived aromatics, they are considered promising bio-based antioxidants, stabilizing reactive oxidized radicals and their derivatives.²⁶ The electron donating *ortho*-methoxy substituents, inherent to lignin's original structure, enhance the radical scavenging ability of the phenolic moiety. Hyperconjugative and inductive effects help to stabilize the phenoxyl radical that is formed after scavenging of an undesired radical.²⁷ Interestingly, a positive effect on antioxidant activity is also found in phenolic compounds having an aliphatic tertiary amine group.^{28–30} Compared to primary and secondary amines, tertiary amines generally have a better oxidative stability.³¹ Moreover, sterically hindered phenolic antioxidants with combined amine functionality are commercially available (e.g., Irganox® MD 1024 and Irganox® 3114 from BASF) and are used in polyolefins to reduce their thermo-oxidative degradation. Unfortunately, they are obtained by a laborious multi-step synthesis, starting from fossil-derived benzene (Figure 1a and Scheme S1).^{32–34} Therefore, selective amination of the aliphatic alcohols in RCF lignin-derived aromatics, while preserving the phenolic moiety, can lead to valuable functionalized antioxidants.

In this contribution, we aim to clarify the phenomena related to the reduced catalytic activity during HB of lignin guaiacol (**1G**) and syringol monomers (**1S**), even in their synthetically pure form, relative to their (non-)phenolic model monomers (e.g., **1H**, 3-(3,4-dimethoxyphenyl)-1-propanol (**1V**)). Appropriate solutions to increase the catalytic activity for **1G** and **1S** are presented, while the developed HB methodology is then successfully used with real refined lignin oil fractions (F_{RFLO}) as shown in Figure 1b. Using a variety of analytical tools (2D HSQC NMR, GC x GC-TOF/MS and GPC), successful amination of not only RCF monomers, but also of the larger dimers is for the first time demonstrated here. In this work, dimethylamine (DMA_n) was chosen as reactant due to its high nucleophilicity, (ii) superior yields in previous work¹⁶, (iii) limited toxicity, (iv) and industrial importance.³⁵ Moreover, the antioxidant capacity of the resulting valuable *N,N*-dimethylamino lignin-derivatives were assessed, supporting their potential as lignin-derived aminated antioxidant agent.

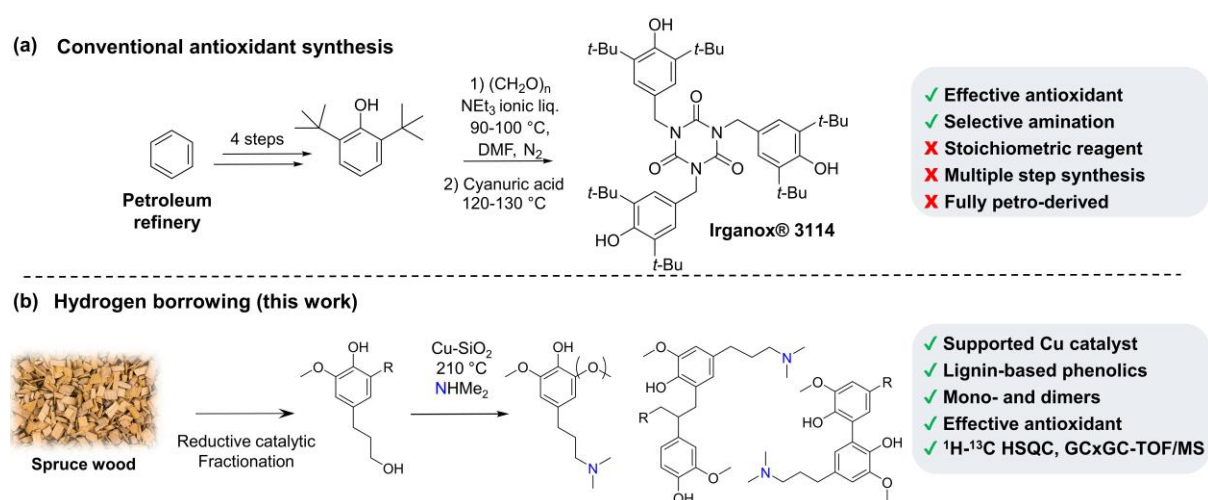


Figure 1. a) Conventional multi-step synthesis of a petro-based antioxidant used in polyolefins with combined phenolic and tertiary amine groups. For detailed synthesis, see Scheme S1. b) Lignin-based phenolic dimethylamines derived from actual lignocellulose by a hydrogen borrowing strategy with antioxidant activity.

EXPERIMENTAL SECTION

Materials

All commercial chemicals were analytical reagents and were used without further purification. For a list of all used chemicals and materials, the reader is kindly referred to the ESI.

Catalyst pretreatment and characterization

During pretreatment, the catalyst (0.12 g) was loaded in a quartz U-tube and a H₂ flow of 60 mL min⁻¹ was established. Temperature was increased (3 °C min⁻¹) to 120 °C and held for 30 min. Next, the temperature was increased (5 °C min⁻¹) to 300 °C and kept for 2 hours. Finally, the catalyst bed was cooled to room temperature (RT, under H₂ flow) before loading into the reaction vessel in ambient air. Cu dispersion was determined via N₂O chemisorption following the procedure reported in literature.¹⁶

Standard reaction procedure

In our standard procedure, a 50 mL stainless steel Parr reactor was charged with 1 mmol **1G**, 0.1 g dodecane internal standard and 20 mL o-xylene solvent, after which 0.12 g of Cu catalyst was added. This corresponded to a total amount of active Cu sites of 7 mol% (Cu-ZrO₂) or 4 mol% (Cu-SiO₂) *versus* the substrate, as measured by N₂O chemisorption. After sealing, the reaction vessel was flushed three times with nitrogen and three times with hydrogen. Then, 2 mmol DMA_n was fed to the reactor using a mass flow controller and the reactor was pressurized with 3 bars of hydrogen and topped of at a total pressure of 10 bar with N₂. A stirring rate of 1400 rpm was applied and the reactor vessel was heated at 6.3 °C min⁻¹ to 210 °C and the reaction time started once the desired temperature was reached. After reaction, the

reaction vessel was cooled to 25°C by an ice-water bath. Next, the reaction mixture and catalyst were collected and the empty reaction vessel was rinsed twice with ethanol, which was collected as well. The catalyst was separated by centrifuging. Next, it was washed a single time with ethanol, which was also collected. The resulting mixture was analyzed by GC-FID and GC-MS.

Product characterization

The identification of the monomeric products was performed with an Agilent GC (6890 series) equipped with a DB17-MS capillary column and an Agilent 5973 series MS detector (scanning range 30-750 g/mol, temperature 320 °C). The inlet temperature was 250 °C. Quantitative GC-FID for monomer analysis was performed on a HP 5890 GC with an Agilent DB-17 column (30 m × 0.32 mm, film thickness of 0.50 µm) and Agilent ChemStation software. 0.2 µL sample was injected at a split ratio of 1:20 with an injector temperature of 250 °C. The FID detector temperature was 320 °C. Quantification was performed by calibration with the pure product against dodecane standard.

Identification of the dimeric and trimeric compounds in the FR_{FLO} before and after amination was done by GC × GC-TOF/MS after derivatization of the samples. The following derivatization procedure was followed: 50 mg of sample was loaded into a GC-vial. Subsequently, 500 µl anhydrous pyridine, 500 µl N-methyl-N-(trimethylsilyl)-trifluoroacetamide and 500 µl of acetonitrile were added. The vial was sealed and put in an oven (80 °C, 30 min). Next, the vial was cooled to 20 °C and analyzed via GC × GC-TOF/MS. The GC x GC comprises a MXT column (60 m × 0.25 mm × 0.25 µm) as the first dimension column connected to a ZB-35HT (2.2 m × 0.18 mm × 0.18 µm) as the second dimension column

through a Sil Tite connection. The column set and a dual-state cryogenic modulator (liquid CO₂) are placed in the same oven. The outlet of the second column is connected to a MS detector. The data acquisition rate was 30 spectra per s with the scanning range set from 6 to 1100 g/mol. The GC x GC-TOF/MS interface (transfer line) temperature was set at 280 °C and the ion source temperature was set at 300 °C. The MS detector used electron ionization (70 eV). Helium was used as carrier gas with constant flow (2.1 ml min⁻¹). The modulation period was optimized (10 s) to obtain maximal resolution in the first dimension without causing wrap-around. The GC system was operated in programmed temperature conditions: 40 °C to 420 °C with a heating rate of 3 °C min⁻¹. Thermo Scientific's XCalibur software was applied and raw data was exported to a .cdf file, subsequently processed by GC Image (Zoex Corporation, USA). The obtained GC x GC-TOF/MS chromatograms are shown in Figures S1.

GPC/SEC analysis of the (aminated) F_{RFO} was performed on a Waters e2695 separations module with a pre-column and a PL-Gel 3µm Mixed-E column with a length of 300 mm, equipped with a Waters 2988 Photodiode array detector (at 280 nm), Empower software and using THF as the mobile phase (1 mL min⁻¹) at 40 °C.

Liquid-phase 1D ¹H and ¹³C NMR and 2D ¹H-¹³C HSQC NMR spectra were acquired on Bruker Avance III HD 400 MHz console with automated samplers. Chemical shifts (δ) are reported in parts per million (ppm) referenced to tetramethylsilane (¹H) or the internal NMR solvent signals (¹³C). In a typical sample preparation, the dried sample (approximately 5 mg for ¹H and 35 mg for ¹³C and 2D HSQC) is dissolved in 500 µL in DMSO-d₆ or MeOH-d₄.

³¹P NMR procedure was used adapted from literature.²³ Each sample was measured in triplicate. A stock solution of anhydrous pyridine and CDCl₃ (1.6:1 vol:vol) was used to make internal standard solution (Cholesterol, 20 mg ml⁻¹) and relaxation agent (Chromium acetylacetonate, 10 mg ml⁻¹). 20 mg of sample was accurately weighed and to this 0.1 ml of the internal standard

solution and 0.05 ml of the relaxation agent solution was added. Next, the phosphitylation agent (2-chloro-4,4,5,5-tetramethyl-1,3,2-dioxaphospholane) was added and mixed thoroughly for 3 minutes before transferring to a clean NMR sample tube. The ^{31}P NMR spectra were obtained on a Bruker Avance 400 MHz NMR, using a standard phosphorous pulse programme (256 scans, 5s interscan delay, O1P 140 ppm). The chemical shifts were calibrated by the peak of residual water and the phosphitylation agent.

ToF SIMS analysis

The Cu-ZrO₂ catalyst surface was analyzed by time of flight secondary ion mass spectrometry (ToF-SIMS) with a ToF-SIMS instrument from IONTOF GmbH as reported previously¹⁶ and described in more detail in the supporting info.

Antioxidant assessment by ABTS assay

Antioxidant properties were analyzed by a 2,2'-azino-bis(3-ethylbenzothiazoline-6-sulfonic acid) diammonium salt (ABTS) assay, a technique commonly used in literature to evaluate phenolic compounds based on UV-vis spectroscopy.³⁶ Hereto, a 7 mM aqueous ABTS solution (Milli-Q water) was prepared and reacted with a 2.5 mM aqueous (Milli-Q water) K₂S₂O₈ solution. The resulting mixture was kept overnight in the dark at 20 °C to generate the final blue-green ABTS^{•+} test solution.³⁷ For the assay, the ABTS^{•+} solution and the (aminated) lignin monomers were dissolved in ethanol, and the UV-vis spectroscopy measurements were carried out on a Shimadzu UV-1800 spectrophotometer. The ABTS^{•+} signal was analyzed at 753 nm and an absorbance value between 0.75 and 1 was found when 40 µl of ABTS^{•+} solution was dissolved in 2 ml absolute ethanol. Upon addition of stock test solutions of (aminated) lignin

monomers at 20 °C, the absorbance signal of ABTS^{•+} at 753 nm was monitored in a kinetic measurement mode for 10 min. Upon addition of antioxidants, discoloration of the ABTS^{•+} solution could be observed, shown by a decrease in absorbance. Quantification was performed by calculation of the ABTS^{•+} signal inhibition after 5 min and 10 min, which was plotted as a function of the antioxidant concentration. Trolox (6-hydroxy-2,5,7,8-tetramethylchroman-2-carboxylic acid), a frequently reported benchmark compound, was used as a reference.²⁶ From this, the IC₅₀ (Half-maximal Inhibitory Concentration) values were obtained, i.e., the concentration of the sample that can scavenge 50% of the ABTS^{•+} free radicals. The Trolox equivalent antioxidant capacity (TEAC) values of all compounds were calculated by dividing the IC₅₀ value of the sample by the IC₅₀ value of Trolox. All measurements were carried out in duplicate.

RESULTS AND DISCUSSION

Hydrogen borrowing of 3-aryl-1-propanols with DMA_n

Our previous work on N-alkylation of DMA_n with lignin model compound 3-(3,4-dimethoxyphenyl)-1-propanol (**1V**) and monomer **1G** using a commercial Cu-ZrO₂ catalyst suggested more harsh reaction conditions for successful lignin monomer amination (**1G**) compared to model compound **1V**. Since **1G** only differs from **1V** by a phenolic hydroxyl group, the influence of oxygenated arene substituents (i.e., methoxy and hydroxy) on the HB reaction rate is assessed firstly. For this, the N-alkylation of DMA_n with six different 3-aryl-1-propanol compounds is compared as displayed in Figure 2. For all six 3-aryl-1-propanol compounds, the tertiary amine **3** was found to be the main product followed by minor amounts of tertiary enamine intermediate **2**. Small quantities of the secondary amine **4** side product were formed, caused by reactant DMA_n disproportionation. Noteworthy, the presence of a phenolic moiety effectively prevents amide (**6**) formation. Possibly the weakly acid phenolic group

favors the formation of enamine **2** over amide **6** starting from the hemi-aminal intermediate **1''** by facilitating water elimination. The substrate conversion rate (r_0) varied between 259 ± 25 to $396 \pm 29 \text{ mM h}^{-1} \text{ g cata}^{-1}$ for the non-phenolic model compounds **1B**, **1A** and **1V** and the phenolic monomer **1H** without a distinct trend. A single hydroxyl or methoxy arene substituent has no noticeable negative effect on the reaction rate. Even the effect of two methoxy groups (**1V**), closely resembling **1G**, is not limiting the alcohol conversion rate. However, a tenfold decrease in alcohol conversion rate was seen for monomers **1G** ($35 \pm 4 \text{ mM} \cdot \text{h}^{-1} \cdot \text{g cata}^{-1}$) and **1S** ($46 \pm 5 \text{ mM} \cdot \text{h}^{-1} \cdot \text{g cata}^{-1}$), potential lignin-derived platform chemicals.³⁸ Thus, only when a phenolic hydroxyl is flanked by an *ortho*-methoxy group, a structural motive inherent to the original structure of the lignin-derived alcohols, it is observed that the substrate conversion rate drops substantially. With the aromatic ring being separated by three aliphatic carbons from the targeted aliphatic primary OH, it is unlikely that the oxygenated arene substituents effect the reaction rate electronically or sterically. Thus, the problematic behaviour of the lignin model monomers **1G** and **1S**, is more likely to be related to interaction of the guaiacyl and syringyl units with the metal and/or oxide support of the Cu-ZrO₂ catalyst.

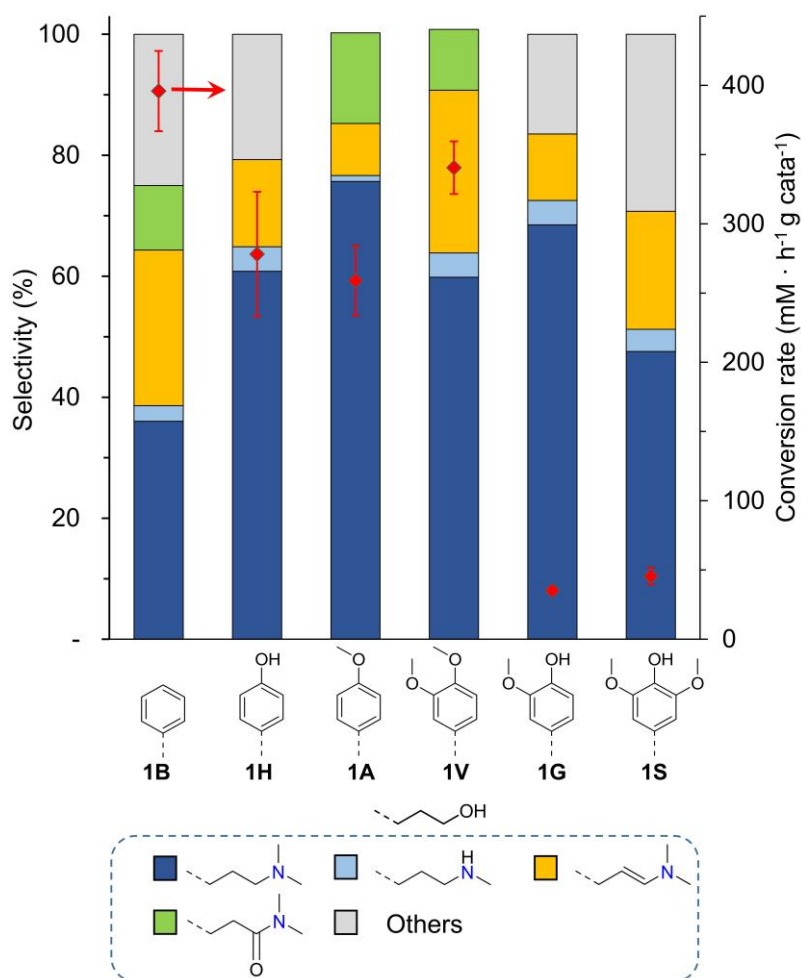


Figure 2. Influence of the aromatic substitution pattern on the hydrogen borrowing amination of various 3-aryl-1-propanol compounds with dimethylamine. Reaction conditions: 1 mmol substrate, 2 mmol DMA, *o*-xylene, 10 bar N₂, 0.12 g Cu-ZrO₂, 190 °C, conversion < 40%. Standard deviations are shown for the conversion rates.

To assess which aromatic substitution pattern is detrimental for the reaction rate, HB of **1V** (as high reactive substrate) with DMA was studied in presence of a fixed amount (20 mol% vs. **1V**) of various guaiacol, syringol and catechol compounds (Figure 3). The additives lack the aliphatic 3-propanol chain in order to restrict the (retarding) effect of the aromatic ring structure to the amination of **1V**, while not being aminated itself. Moreover, using a fixed substrate (**1V**) allows facile comparison of substrate conversion rate between different additives. For all reactions with additives, no new reaction products were detected and mass balances for **1V** remained nearly closed, implying no additional side reactions took place. Lignin monomers

1G and **1S** are known radical scavengers (i.e., antioxidant) due to their hindered phenolic moiety. If any radical process occurs during HB, the presence of a radical scavenger could hinder the reaction. Therefore, butylated hydroxytoluene (BHT, Entry 2), a commonly used sterically hindered radical scavenger³⁹ was added as control experiment. No noticeable change in the values of r_0 was observed, thereby excluding reaction inhibition due to radical trapping during HB. Next, various methoxylated phenolics were examined (entry 3-6). Clearly, all compounds had a pronounced retarding effect on the values of r_0 , with guaiacol (entry 6) having the largest impact. Relative to guaiacol, adding a *para*-propyl chain (entry 4) or moving the *ortho*-methoxy group to *meta* position (entry 5) to the phenolic OH, showed slightly less impact on the initial reaction rate. Syringol (entry 3), having two *ortho*-methoxy, was less troublesome for the reaction compared to guaiacol, which is in agreement with the results in Figure 2 (HB amination of **1G** versus **1S**). These findings suggest that on one hand the rate-hindering effect of methoxyphenols diminishes with increasing steric hindrance of the phenolic OH. On the other hand, an *ortho* -OCH₃ substitution relative to the phenolic -OH has the largest effect of the di-substituted arenes. The reduced values of r_0 might be related to the adhesive interactions of guaiacol and syringol with the catalyst surface. For this reason, (*o*-methoxy)catechol derivatives were examined (entry 7-9), as they are known to exhibit exceptionally strong adhesion capacities with various surfaces⁴⁰. A drastic decrease for the values of r_0 was indeed noticed when catechol (entry 9) or its derivatives (entry 7-8) were added to the reaction mixture, blocking **1V** conversion nearly completely. Adding sterically hindrance (entry 7 and 8) to catechol did limit its rate inhibition ability slightly.

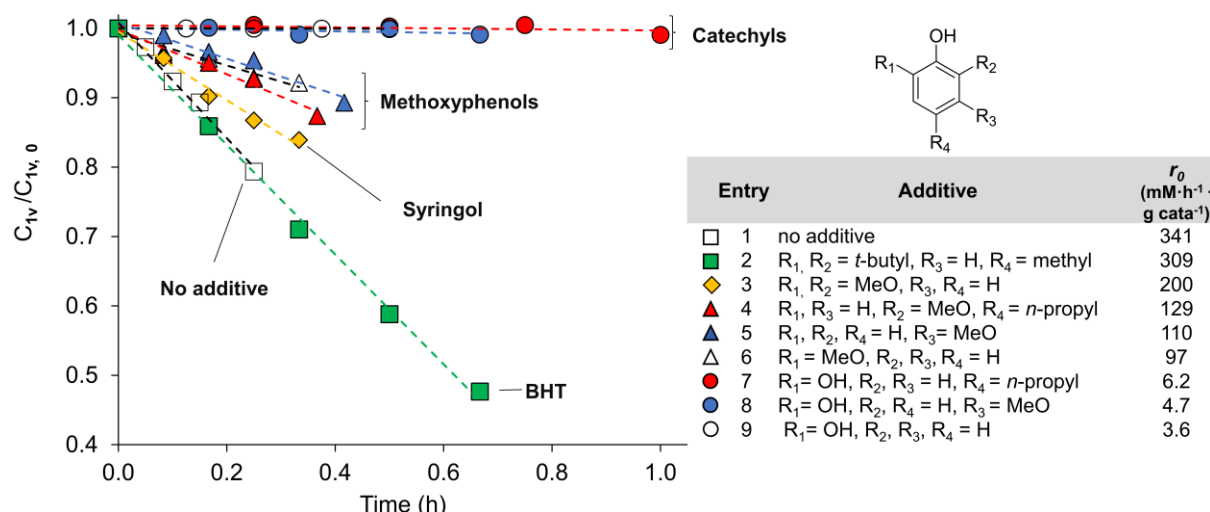


Figure 3. Kinetic plots for the HB of **1V** towards tertiary amine **3V** in the presence of various additives. The normalized **1V** concentration (vs. $\mathbf{1V}_{t=0\text{ h}}$) is given as a function of the reaction time. For the initial conversion rate (r_0), the slope of the linear fit (generally $R^2 > 0.95$) through the initial points of the **1V** concentration were calculated. Conversion < 20%, except for BHT (green squares). Reaction conditions: 1 mmol **1V**, 0.2 mmol additive, 2 mmol DMA, *o*-xylene, 10 bar N_2 , 0.12 g Cu-ZrO₂, 190 °C,

The role of catechol-derivatives during hydrogen borrowing amination

Catechol and guaiacol only differ by one methoxy group. O-demethylation of **1G** or **1S** (or their aminated products) under the HB reactions conditions would lead to strongly deactivating catechol derivatives, structurally similar to 4-propylcatechol (Figure 3, entry 7) as proven in the previous section. Water is formed as by-product during HB and in the presence of the acidic sites of the ZrO₂ support, O-demethylation of the methoxy group can take place to yield catechol derivatives that strongly adsorb on the surface.⁴¹ Alternatively, cleavage of the PhO-CH₃ bond in anisole on a zirconia has been reported in absence of water at temperature ranging from 150-300 °C, forming phenolate and CH₃ species adsorbed on the surface.⁴²

Indeed, during HB of **1G** with DMA, trace amounts of 4-(3-hydroxypropyl)benzene-1,2-diol (catecholpropanol) could be detected by GC-MS (<0.5 wt%) (Figure S6) proving O-demethylation takes place. As demonstrated in a control experiment, catechol strongly adsorbs on the Cu-ZrO₂ catalyst, also complicating its detection by GC-FID (Figure S2). To assess the

extent to which catechol derivatives inhibits the HB reaction, catechol was deliberately added in varying concentration (0-14 mol% *versus* substrate) to the reaction mixture during HB of **1H** with DMAc. Here, **1H** was chosen as lignin model to ensure no additional O-demethylation of the substrate could take place. As the applied Cu-ZrO₂ catalyst has a specific number of Cu active sites (0.6 mmol · g⁻¹ catalyst) as measured by N₂O chemisorption, the catechol concentration was also displayed relative to the number of active Cu sites. From Figure 4 it is evident that very low levels of catechol (2-3 mol% *vs.* **1H**, <200 ppm) are sufficient to drastically reduce **1H** conversion from 90% to 20%. In fact, 0.5 catechols per active Cu is sufficient to radically reduce the rate. Increasing the catalyst loading (0.2 g *versus* 0.12 g), thereby changing the catechol-to-active Cu sites ratio, followed the same trend line, indicating that catechol blocks the active reaction sites for HB.

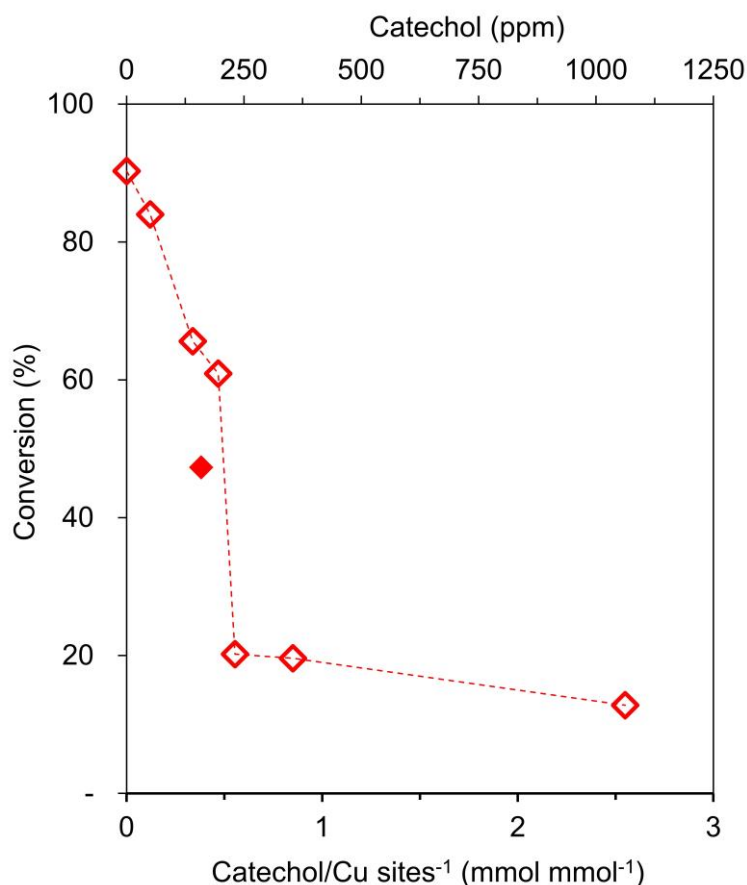


Figure 4. Influence of catechol concentration on the HB of **1H** with DMAn. The amount of catechol is expressed relative to the amount of surface Cu sites as measured by N₂O chemisorption. The dashed line is merely a guide to the eye. Reaction conditions: 1 mmol **1H**, 2 mmol DMAn, 0.12 g (empty diamonds) or 0.2 g (filled diamond) Cu-ZrO₂, *o*-xylene, 190 °C, 4h, 10 bar total pressure.

ToF-SIMS analysis

The pretreated and spent Cu-ZrO₂ catalyst obtained after HB reactions was analyzed by ToF-SIMS. This technique has proven itself of great value during the characterization of heterogeneous catalyst surfaces owing to its exceptional sensitivity for organic and inorganic surfaces species.^{43–46} Here, we obtained ToF-SIMS spectra of different Cu-ZrO₂ catalysts after HB of **1H** and **1G** with DMAn to assess the influence of (i) low pressure hydrogen during reaction, (ii) the phenol substrate, and (iii) catechol derivatives (Table 1). The total intensities of various Cu and Zr cations detected in ToF-SIMS (obtained from Cu and Zr surface species with various oxidation states after bombardment with Bi₅⁺ and ionization) are shown in Table

1. These intensities are used as proxy to quantify the actual Cu and Zr species at the outermost surface of the catalyst. A full list of all detected species is provided in Table S1. Pristine Cu-ZrO₂ catalyst, pretreated with H₂ at 250 °C was used as benchmark (entry 1). Hydrogen was included as a factor in this analysis as previous work appointed hydrogen as a key parameter for both high conversion and tertiary amine selectivity.¹⁶ Comparison of the Cu surface species after HB of **1G** in absence (entry 2) and presence (entry 3) of hydrogen showed a decline relative to the pretreated Cu-ZrO₂ (entry 1) for both conditions. A stronger decline is observed in Cu surface species when no hydrogen pressure is applied. As opposed to the surface Cu species, hydrogen had no effect on the surface Zr species.

The HB of **1H** and **1G** with DMA_n by Cu-ZrO₂ showed a clear difference in initial substrate conversion rate (Figure 2). Moreover, to obtain similar substrate conversion levels for both substrates, more harsh conditions were applied for **1G** (16h, Table 1 entry 3) relative to **1H** (5h, Table 1 entry 4). Assessment of the Cu surface species shows a similar decrease for both substrates after HB relative to pristine Cu-ZrO₂ (entry 1). On the contrary, the amount of Zr surface species on the Cu-ZrO₂ catalyst surface remains constant after HB with **1H**, whereas a large decrease is seen after HB of **1G**. Consistently, the Cu/Zr ratio sharply rose after reaction with **1G**, whereas a minor decrease was noticed for **1H**. These results indicate that accumulation of **1G** derived species is occurring preferentially on the Zr surface species.

Assessment of the organic species on the catalyst surface by ToF-SIMS was done to further clarify the nature of the fouling. To simplify the analysis, the pool of detected organic fragments were divided in categories: aminated (C_xH_yN_z⁺), oxygenated (C_xH_yO_z⁺), alkanes (C_xH_y⁺) and fragments with more than 12 carbons (C₁₂⁺). The latter as an arbitrary indicator for high molecular weight products. A full list of all detected cations can be found in Table S1. An increase by more than an order of magnitude in aminated species on the catalyst surface is

found after HB, with a factor 23 increase for **1G** (entry 3) and a factor 11 increase for **1H** (entry 4) relative to benchmark catalyst (entry 1). An increase in aminated species on the catalyst surface was also found in our previous work during catalyst recycling experiments after HB of **1V** with Cu-ZrO₂.¹⁶ The high abundance of aminated species, even after three washing steps and drying of the catalyst prior to ToF-SIMS analysis indicates their high affinity for the catalyst surface, especially those derived from **1G**. Species derived from **1G** and **1H** are found on the catalyst surfaces after reaction, as illustrated by the elevated intensity of the 4-guaiacolmethylium cation ($C_8H_9O_2^+$) and the 4-phenolmethylium cation ($C_7H_7O^+$), respectively.

Working under low hydrogen pressure has no pronounced effect on the aminated species on the catalyst surface, however it reduces the intensity of C₁₂₊ surface species by a factor four. Noteworthy, a higher abundance of C₁₂₊ surface species was found after HB with **1H**. As excellent **1H** conversion at a short reaction time (5 h) was obtained, the presence of the C₁₂₊ species after reaction cannot explain the lower **1G** conversion rate. Neither the oxygenated species ($C_xH_yO_z^+$), nor the alkanes ($C_xH_y^+$) showed a distinct trend for the various reaction conditions. The results thus reveal that the detected 4-guaiacolmethylium cation suggests strong adsorption of **1G** derivatives, which is preferentially taking place on the zirconia support as indicated by the increased Cu/Zr ratio after reaction. As a consequence, the reduced catalytic activity of Cu-ZrO₂ for **1G** can be linked to this fouling of the Zr surface species. As a control experiment, catechol (20 mol% *versus* **1H**) was intentionally added to a HB reaction of **1H** with Cu-ZrO₂, causing a drastic reduction in alcohol conversion (Table 1, entry 5). Even after three washing steps, residual catechol species are detected on the catalyst surface (Table 1, $C_6H_5O_2^-$) emphasizing its high affinity for the catalyst surface. The intensity of Cu⁺ and Zr⁺ cations decreased, however the Cu⁺/Zr⁺ ratio remained stable compared to the pretreated Cu-

ZrO₂ catalyst (entry 1). Catechol thus affects both Cu and Zr surface species. The addition of catechol results in an increase in higher molecular weight fragments (C₁₂₊). Polymerization of catechol to form metal chelating polymers is known to occur easily at room temperature, and can be catalyzed by Cu species.⁴⁷ O-demethylation of methoxyphenols to yield catechols should thus be avoided in order to preserve the surface Cu and Zr species.

Table 1. Normalized intensities obtained by ToF SIMS on the Cu-ZrO₂ catalyst surface after HB of **1G** and **1H** with DMAc. The fragments are summed up in categories. Detected intensities are normalized by dividing by total cation count minus the Na⁺ intensity (for anions: total anion count minus the H⁻ intensity). Each sample was analyzed on three different spots. The average with standard error is reported. A full list of detected cations is provide in ESI Table S1.

Entry	1	2	3	4	5
Substrate ^a	None	1G	1G	1H	1H
H ₂ pressure (bar)	-	0	1	1	1
Additive ^d	-	-	-	-	Catechol
Conversion (%)	-	73 ^b	86 ^c	97	27
Selectivity ^e (%)	-	62	68	89	44
ToF SIMS normalized intensities (± SD) ^f					
Total Cu ⁺ (x 10 ⁻²)	21.3 ± 0.4	5.9 ± 0.1	12.0 ± 0.2	12.0 ± 0.1	7.2 ± 0.2
Total Zr ⁺ (x 10 ⁻²)	6.1 ± 0.2	0.77 ± 0.03	0.6 ± 0.2	6.33 ± 0.09	2.4 ± 0.3
Cu ⁺ /Zr ⁺	3.5 ± 0.1	7.7 ± 0.2	18.4 ± 0.6	1.90 ± 0.03	3.0 ± 0.3
C _x H _y N _z ⁺ (x 10 ⁻²)	0.41 ± 0.01	6.8 ± 0.6	9.38 ± 0.06	4.5 ± 0.1	3.5 ± 0.2
C ₁₂₊ ⁺ (x 10 ⁻³)	0.43 ± 0.02	4.6 ± 0.1	1.22 ± 0.04	4.37 ± 0.02	8.3 ± 0.5
C _x H _y O _z ⁺ (x 10 ⁻²)	4.7 ± 0.2	4.7 ± 0.2	4.92 ± 0.03	5.1 ± 0.5	2.8 ± 0.1
C _x H _y ⁺ (x 10 ⁻²)	8.49 ± 0.07	5.3 ± 0.2	6.93 ± 0.03	6.72 ± 0.08	3.1 ± 0.05
C ₈ H ₉ O ₂ ⁺ (x 10 ⁻³)	0.027 ± 0.004	3.12 ± 0.03	0.70 ± 0.02	0.096 ± 0.005	-
C ₇ H ₇ O ⁺ (x 10 ⁻³)	0.20 ± 0.02	0.84 ± 0.04	0.89 ± 0.01	5.2 ± 0.3	1.17 ± 0.06

$\text{C}_6\text{H}_5\text{O}_2^- (\times 10^{-3})$ 0.050 ± 0.002 1.3 ± 0.1 0.46 ± 0.01 0.46 ± 0.02 10 ± 1

a) Reaction conditions: 1 mmol substrate, 2 mmol DMAAn, *o*-xylene, 0.12 g Cu-ZrO₂, 10 bar total pressure (H₂ + N₂), 5 h, 190 °C. b) 48 h, c) 16 h, 190 °C. d) 0.2 mmol, e) Selectivity towards tertiary amine **3G** and **3H** for **1G** and **1H**, resp. f) Cu-ZrO₂ catalyst obtained after reaction was washed thrice with EtOH and dried at 80 °C prior to analysis.

The effect of hydrogen

As shown by ToF-SIMS and in our previous work, hydrogen is of key importance to reach high substrate conversion rates and increase the tertiary amine product selectivity.¹⁶ Therefore, once again we performed the HB of lignin monomer **1H** with DMAAn in presence of catechol (Figure 4), but this time with 1 bar of hydrogen pressure (Figure 5). The addition of a small amount of hydrogen partly negates the detrimental effect of catechol with improved **1H** conversions for all catechol concentrations. Alcohol conversion levels also benefitted from low-pressure hydrogen as it helps to keep the catalyst in its active state, likely by *in situ* regeneration of the active catalyst after deactivation.⁴⁸ Consequently, the hydrogen pressure was optimized for the HB of **1G** with DMAAn (Figure S3). Overall, the optimal conditions found for HB of **1G** with DMAAn were temperature of 210 °C, an initial hydrogen pressure of 3 bar and a reaction time of 16h. This resulted in an optimal conversion of **1G** of 86% with a selectivity of tertiary amine **3G** of 91%.

Alternative catalyst support

ToF SIMS analysis revealed a pronounced decrease of the surface Zr species after the HB of lignin monomer **1G** with DMAAn. The nature of the catalyst support could influence the adhesion strength between catalyst and substrate, as well as the extend of methoxyphenol O-demethylation to catechol. For instance, phenol, anisole and guaiacol are reported to mainly interact via H-bonding with a silica support, whereas on alumina stronger chemisorption is

reported.^{42,49} Phenol and guaiacol are found to adsorb as (double) phenolate species with the amount being directly dependent on the Lewis acidity of the support. ZrO₂ has weak Lewis acid and basic sites that form stable phenolate species.^{42,49} Whereas interaction of the substrate with the support is required to enable reaction, strong chemisorption or incorrect orientation of the substrate can impede catalysis or can lead to undesired surface reactions due to the long residence time. For this reason, we additionally tested two commercial Cu catalysts (Sponge Cu and Cu-SiO₂) and one Ni catalyst (Raney Ni) with less acidic/basic surface properties or no oxide support for the HB of **1G** with DMA_n under the optimized conditions (Table S2). Whereas Raney Ni on the one hand displayed a high conversion (98%), selectivity for the tertiary amine was unsatisfying (49%). On the other hand, sponge Cu displayed good tertiary amine selectivity (78%), but with only moderate conversion (50%). Interestingly, Cu-SiO₂ reached identical conversion of **1G** (86%) relative to Cu-ZrO₂, but stands out with excellent selectivity towards tertiary amine **3G** (97%). Aiming at explaining the better performance, ToF SIMS analysis of the Cu-SiO₂ catalyst before and after amination of **1G** with DMA_n was performed (ESI Table S3). The resemblance with the ToF SIMS results for Cu-ZrO₂ is noteworthy, with trends being very similar when comparing the relative changes (*versus* the blank catalysts) in terms of Cu, Si (or Zr for Cu-ZrO₂ catalyst) and **1G**-derived surface species. This is in good agreement with the identical substrate conversion levels obtained for both catalysts under the applied conditions. However, for Cu-SiO₂, the relative increase in intensity of nitrogen containing cations ($C_xH_yN_z^+$) is approximately three times smaller compared to the Cu-ZrO₂ catalyst. This suggests a lower affinity of the present amines for the Cu-SiO₂ catalyst surface, which can be attributed to the less pronounced surface acidity of SiO₂ compared to ZrO₂.^{50–52} As a consequence, a decrease in side reaction involving amines (e.g., alkylamine disproportionation) could explain the higher selectivity for the Cu-SiO₂ catalyst.

To assess the influence of catechol on the Cu-SiO₂ catalyst, amination of **1H** with varying catechol-to-active Cu sites ratio was performed (Figure 5). Under the same conditions as for Cu-ZrO₂, conversion of **1H** for Cu-SiO₂ (81%) in absence of catechol was somewhat lower compared to Cu-ZrO₂ (97%), likely due to the lower total amount of active Cu sites on mass basis (0.35 *versus* 0.61 mmol · g⁻¹, resp.). Nevertheless, Cu-SiO₂ activity was much less affected by catechol, as its activity holds even at the high catechol concentrations (i.e., high catechol-to-active site ratio). Silica lacks strong acidic groups and basic sites, thus showing lower affinity for phenolic species, in particular catechol derivatives. Although acidic and basic sites are generally considered beneficial for HB,¹⁸ here we demonstrate that for lignin monomer **1G**, a silica support with less pronounced acidity/basicity surface properties performs substantially better.

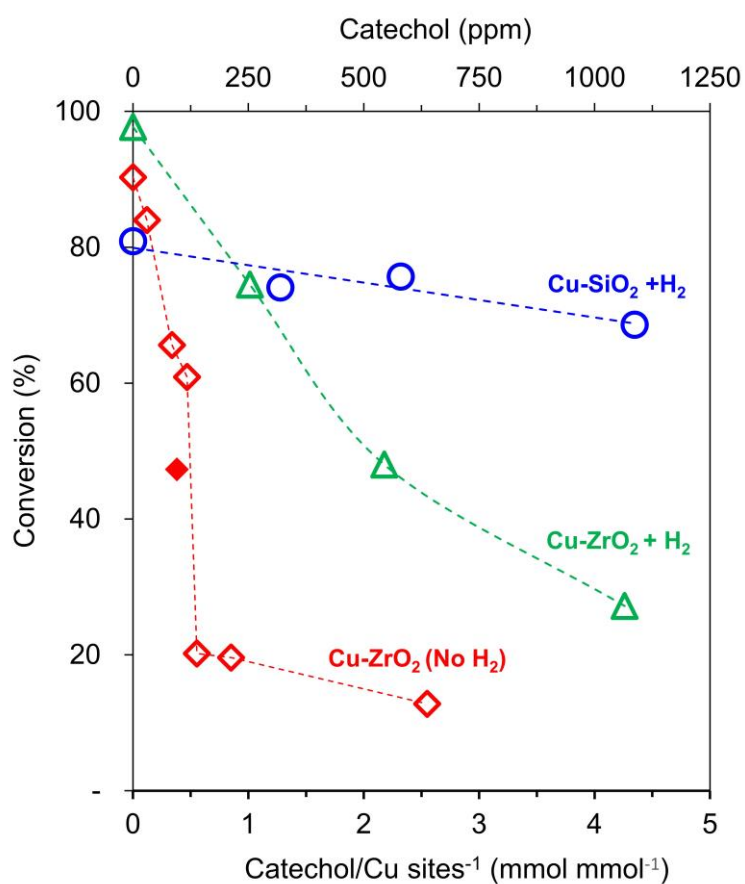


Figure 5. Influence of catechol concentration on the HB of **1H** with DMA_n by Cu-ZrO₂ (◆, △) or Cu-SiO₂ (○) with 1 bar H₂ (△, ○). The amount of catechol is expressed relative to the amount of surface Cu sites as measured by N₂O chemisorption for Cu-ZrO₂ (0.61 mmol Cu sites/g) and Cu-SiO₂ (0.35 mmol Cu sites/g) catalysts. The dotted line is merely a guide to the eye. Reaction conditions: 1 mmol **1H**, 2 mmol DMA_n, 0.12 g (empty diamonds) or 0.2 g (filled diamond) Cu-ZrO₂, *o*-xylene, 190 °C, 4h, 10 bar total pressure (N₂ + H₂).

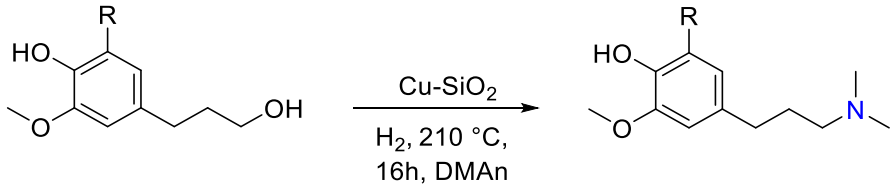
Hydrogen borrowing of real RCF lignin fractions

With Cu-SiO₂, superior tertiary amine **3** yields for dihydroconiferyl alcohol (83%) and dihydrosinapyl alcohol (84%) with dimethylamine were obtained (Table 2). As a first control experiment, the stability of the tertiary *N,N*-dimethylamino product was assessed under reaction conditions (Figure S4). No significant product degradation for tertiary amine **3S** was observed after 24h at 210 °C in presence of dimethylamine and Cu-SiO₂. Moreover, after storing the isolated tertiary amine products (**3P**, **3S**) for more than six months under ambient atmosphere at room temperature, no degradation products could be identified. As a second series of control experiments, the Cu-SiO₂ catalyst stability was evaluated. Good catalyst reusability upon recycling was found with limited loss in catalytic activity after four reaction cycles (See Figure S5).

With both product and catalyst being stable, applying the Cu-SiO₂ HB methodology on real RCF lignin streams is an evident next step to take. For this, a benchmark RCF reaction was performed on a 2 L scale using spruce lignocellulose and a Pd/C catalyst. Under these conditions, a high selectivity towards propyl alcohol end groups (Figure 6a) is obtained.²⁰ Here, 150 g of spruce sawdust, 15 g of Pd/C and 800 mL of MeOH were added to a 2 L Parr reactor. The reactor was pressurized with 30 bar H₂, heated to 235 °C while stirring at 600 rpm. After

a reaction time of 3 h, the reactor was cooled and the mixture was filtered, followed by an EtOAc-water extraction to wash out the sugars, to obtain the refined lignin oil (RFLO).

Table 2. Tertiary amines via hydrogen borrowing amination of RCF lignin monomers and RCF lignin oil fraction and with DMAc



Substrate	Conversion (%)	Selectivity (%)	Yield (%)
1G (R = H)	86	97	83
1S (R = OMe)	94	89	84
1G RFLO" (b)	84	68	57

a) Reaction conditions: 1 mmol substrate, 2 mmol DMAc, *o*-xylene, 0.12 g Cu-SiO₂, 3 bar H₂, 16h, 210 °C. b) 0.28 g fractionated lignin oil, corresponding to 0.7 mmol **1G**, and 0.24 g Cu-SiO₂

A stable RCF lignin oil was obtained representing 56 wt% of the Klason lignin content, with a high degree of depolymerization as proven by the phenolic monomer yield (33 wt% in the oil). Within the monomer fraction, a high selectivity to **1G** (85%) was obtained. Additionally, minor amounts of 4-(3-methoxypropyl)guaiacol and 4-alkylguaiacols (propyl, ethyl and methyl) were observed (Figure 6a), consistent with literature for softwood RCF.²³ To increase the content of dihydroconiferyl alcohol, the original refined lignin oil was extracted twice with heptane/ethyl acetate (70/30 vol%). The second extract was chosen, hereafter referred to as refined lignin oil double prime, F_{RFLO"}, for further amination as it was significantly enriched in **1G** monomer (45

wt% of the fraction) and was stripped off possible disruptive extractives (e.g., terpenes and fatty acids).

The F_{RFLO} fraction also contains 50 wt% of dimers and oligomers, as illustrated by GC-FID and GPC (Figure 6b, c). The insoluble residue after heptane/ethyl acetate extraction can be used as valuable raw material for polymers applications, such as printing ink and lubricants.^{53,54} Next, the Cu-SiO₂ based amination protocol was applied to F_{RFLO} , resulting in a high conversion of 84% of the present **1G** and a decent yield of 57% towards tertiary amine **3G** (based on the initial **1G** content, by GC-FID). The GPC chromatogram (Figure 6c) shows a shift to higher retention time for the tertiary amine monomer **3G** relative to **1G**. Although this suggests a lower hydrodynamic volume for the amine product, additional interaction between the GPC column material and the tertiary amine, thereby effecting the retention time, cannot be ruled out.⁵⁵ A similar shift to lower apparent M_w is seen for the dimers and oligomers in the aminated F_{RFLO} , suggesting some amination has taken place in these fractions.

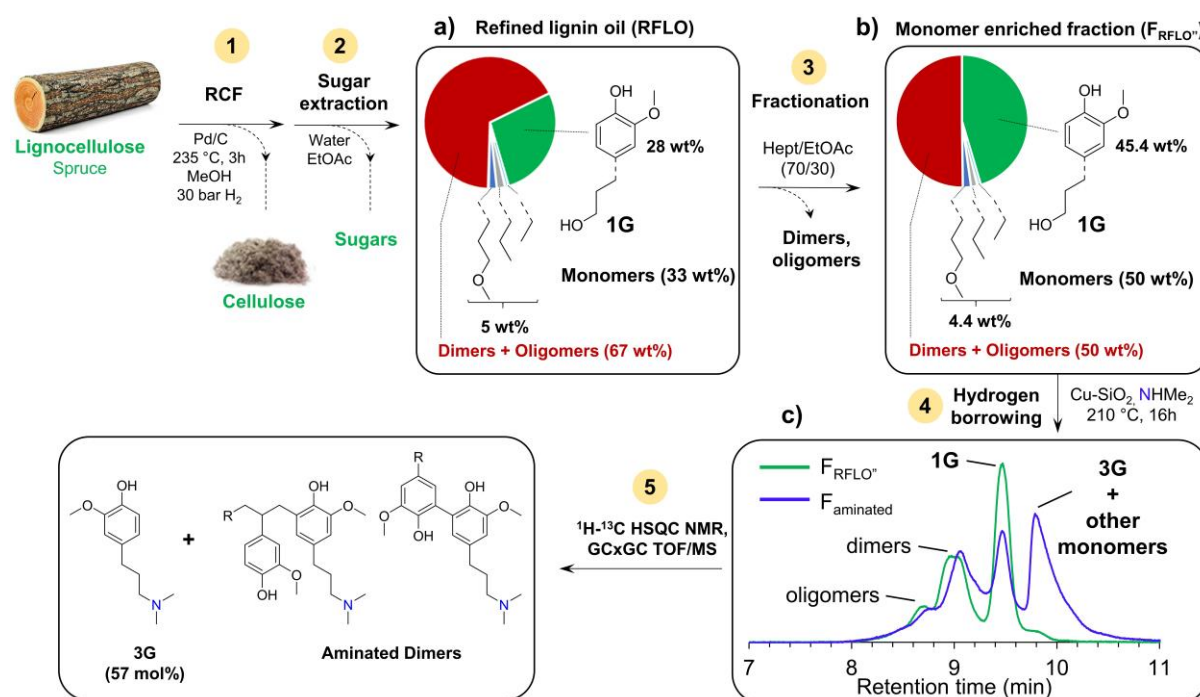


Figure 6. An integral approach to obtain aromatic alkyl amines directly from RCF fraction of lignocellulose. RCF of spruce wood gives crude RCF lignin oil and a cellulose pulp. Sugar

extraction delivers a RFLO with typical composition a) as measured for the refined RCF oil and b) the fractionated F_{RFLO} . c) HB of F_{RFLO} with DMA n and the Cu-SiO $_2$ catalyst, yields the desired tertiary amine **3G** and aminated dimers as shown in the GPC/SEC chromatogram. Reaction conditions: 0.28 g F_{RFLO} , 4 mmol DMA n , *o*-xylene, 0.24 g Cu-SiO $_2$, 3 bar H $_2$, 16h, 210 °C.

Relative quantification *via* 2D HSQC NMR is an excellent techniques to give detailed structural information for the entire F_{RFLO} and its aminated product.^{23,24,56} The main advantage of this technique is that it allows to quantify the total relative abundance of a specific inter-unit or end-unit for an entire RCF mixture (i.e., for mono-, di- and oligomers). This is due to the limited amount of C-H correlating signals for a certain end- or interlinkage unit, independent of the individual molecular structure. Therefore, conversion of the different inter-unit and end-unit OH's can be verified, hereby using the aromatic G2 area as internal standard (Table 3). To calculate the conversion of all γ -propanols (γ -POH) in the end-units, the β C-H signal of the γ -POH moiety was monitored before and after amination. To reduce processing errors, the manual integration of the data has been done in triplicate. Comparing γ -POH (end-units) before and after amination gave a conversion of 72%, which is slightly lower than the **1G** monomer conversion (84%) measured by GC-FID. Thus, the end-unit γ -POH groups in dimers and oligomers seemingly have a somewhat lower reactivity compared to monomers, but they are reactive for HB amination. An excellent selectivity of 93% towards γ -PNMe $_2$ was found. Looking at the alcohol moieties situated on the inter-units of dimers and oligomers, a minimal conversion in total inter-unit hydroxyls is found (Table 3), suggesting that the end groups are more reactive, likely due to lower steric hindrance and better surface interaction at the active site of the Cu catalyst. A small decrease in β - β 2x POH and β -5 POH signal suggests amination of the inter-unit OH has taken place here, whereas the level of β -1 POH remain quasi constant, and can be considered unreactive. Overall, a combined end- and inter-unit POH conversion of 70% is found by 2D-HSQC NMR.

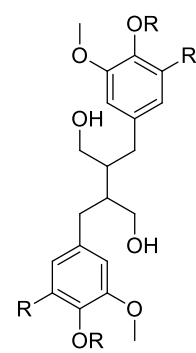
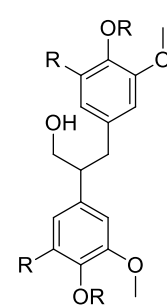
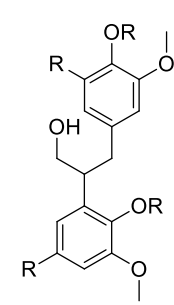
A frequently applied method to assess the aliphatic and phenolic OH content is ^{31}P NMR, after phosphorylation of the sample with 2-chloro-4,4,5,5-tetramethyl-1,3,2-dioxaphospholane. The results of the ^{31}P NMR measurements (in triplicate) are summarized in Table 3, before and after amination of the F_{RFLO} . A high total hydroxyl content of $8.5 \text{ mmol OH g}^{-1}$ was found for the F_{RFLO} of which the phenolic OH content was $4.5 \text{ mmol OH g}^{-1}$ and the aliphatic $4.0 \text{ mmol OH g}^{-1}$, which are expected values for fractionated RCF lignin oil from softwood.²³ After amination, the phenolic OH content did not change significantly, being $4.2 \text{ mmol OH g}^{-1}$, showing the phenolic hydroxyl remains unaffected by the HB protocol and thus available for additional upgrading. In contrast, the total aliphatic hydroxyl content decreased to $1.0 \text{ mmol OH g}^{-1}$, which represents a 76% conversion of the aliphatic hydroxyl groups. This is in fair agreement with the 70% conversion of aliphatic OH (end- and inter-unit OH) obtained by semi-quantitative 2D HSQC NMR and proves both techniques are complementary.

In order to further elucidate the individual molecular structure of the dimers and trimers, high resolution GC x GC – TOF/MS was used in addition to GC-MS, as a state of the art technique to analyze RCF lignin oil.²⁴ To identify the RCF dimers and trimers, the obtained deconvoluted MS spectra were compared to literature. Since this technique has - to the best of our knowledge – never been used to analyze amine-functionalized lignin oil, compounds were assigned based on their mass fragmentation patterns (Figure S7-S25). The chromatographic image of F_{RFLO} before and after amination with DMA_n using Cu-SiO₂ were obtained (Figure S1) and the identified structures are shown in Figure 7. Beside the already identified monomers, a total of 13 dimers were identified in F_{RFLO} . No trimers were observed, since fractionation with heptane/ethyl acetate (70/30) does not readily extract trimers from the RFLO, as previously suggested.²⁴ Although some oligomers (with $M_w >$ trimers) are extracted from the RFLO, as

illustrated by GPC (Figure 6c), these compounds are not sufficiently volatile to be detected by the (GC x) GC technique.

Figure 7a shows all detected dimers having a γ -POH group on the end-unit (**D1**, **D4**, **D7-D9**), inter-unit (**D5**, **D11**, **D12**), on both end- and inter-unit (**D2**, **D10**) or without a γ -POH group (**D3**, **D6**, **D13**). The latter ones have no aliphatic alcohol and therefore are not susceptible to amination. After HB of F_{RFLO}'' with DMA_n, a total of 6 dimers (**A1-A6**) containing a tertiary amine group were identified (Figure 7b). In the deconvolution of the mass spectra, a signature m/z of 58 signalled the incorporation of DMA_n into the dimer, caused by α -cleavage of the tertiary amine during fragmentation. In line with the NMR results, amination took preferably

Table 3. Integration results of 2D HSQC and ^{31}P NMR of fractionated lignin oil (F_{RFLO}'') and the same fraction after amination with DMA_n (F_{DMA_n}).^a Samples are obtained in triplicate with average shown and standard deviation between brackets.^b

 <p>β-β 2x POH</p>	 <p>β-1- POH</p>	 <p>β-5 POH</p>
	F_{RFLO}''	F_{DMA_n}
End-unit		
γ -POH	54.6 (1)	15.4 (0.7)
γ -PNMe ₂	0	36.3 (3)
Inter-unit		
β - β 2x POH	0.7 (0.1)	0
β -1 POH	1.60 (0.04)	1.4 (0.2)

β -5 POH	1.6 (0.2)	0.7 (0.2)
Total inter-unit POH	3.9 (0.3)	2.2 (0.4)
<hr/> ³¹P NMR		
Aliphatic OH (mmol g ⁻¹)	4.0 (0.1)	1.0 (0.1)
Phenolic OH (mmol g ⁻¹)	4.5 (0.1)	4.2 (0.4)
Total OH (mmol g⁻¹)	8.5 (0.2)	5.2 (0.4)

(a) Reaction conditions: 0.28 g F_{RFLO}, 4 mmol DMA_n, *o*-xylene, 0.24 g Cu-SiO₂, 3 bar H₂, 16h, 210 °C. (b) For 2D HSQC, the semi-quantification is relative to the G₂ area of the corresponding spectra and expressed as per 100 G₂ units.

place on the end-unit POH, with the inter-unit hydroxyls remaining unaffected. 2D HSQC NMR showed a very small decrease in inter-unit γ -POH content after amination, possibly hinting at inter-unit POH conversion. This could be related to the errors associated with semi-quantitative HSQC or simply concentrations that were below the detection limit of the GC x GC. Although tertiary diamines can be formed in case of diols (e.g., **D2**, **D10**, **D11**), only mono amino alcohol were found (**A1-A6**). For the detected compounds in F_{RFLO} with a β - β or β -1 inter-unit (**D11**, **D12**), no aminated product could be detected, probably because they lack an end-unit γ -POH. Overall, these results prove that Cu-SiO₂ is an effective catalyst for HB of both lignin mono- and dimers with a preference for end-unit γ -POH in dimers. The high selectivity for end group amination, allows for further functionalization of the remaining OH

groups,

e.g.

propoxylation

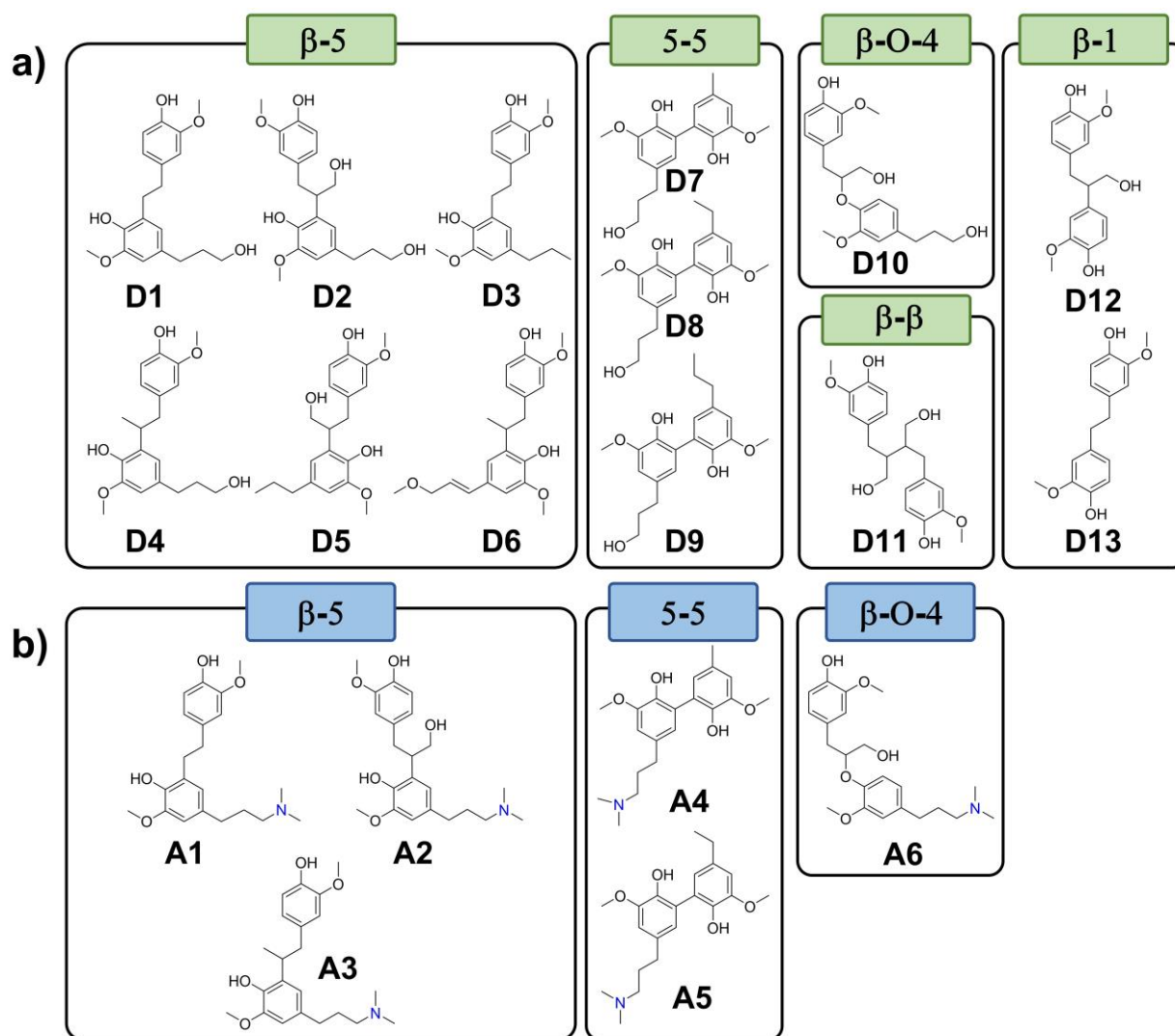


Figure 7. Structures of observed (a) dimers in F_{RFO} and (b) aminated dimers products detected by (GC x) GC-MS after HB of F_{RFO} with DMAn by Cu-SiO₂. Reaction conditions: 0.28 g F_{RFO} , 4 mmol DMAn, *o*-xylene, 0.24 g Cu-SiO₂, 3 bar H₂, 16h, 210 °C.

or glycidylation among other options.^{57,58}

Evaluation of antioxidant capacity

Amine containing hindered phenolics form a unique group of antioxidants. The presence of both functionalities in a single molecule allows for a synergetic effect on antioxidant activity.^{28–}

³⁰ For example, a commercial antioxidant additive is Irganox® 3114 from BASF, commonly used to avoid thermo-oxidative degradation of polyolefins.³⁴ Here, the antioxidant activity of

the lignin monomers and their aminated derivatives is assessed. The Trolox equivalent antioxidant capacity (TEAC) assay is a commonly used standard method to evaluate the antioxidant activity of phenolic compounds, having the advantage of simple operation, wide working pH, and rapid reaction between the radical and the antioxidant agent.⁵⁹ During this assay, the ability of the antioxidant to scavenge the stable radical cation ABTS^{•+} is tested. The ABTS^{•+} radical is a chromophore, while the neutralized ABTS molecule is colorless, therefore allowing the scavenging process to be monitored by UV-VIS spectroscopy. The antioxidant capacity of a compound is quantified by the TEAC values, where a TEAC value smaller than one represents a compound with a larger antioxidant capacity than Trolox. The total antioxidant capacity of the lignin monomers **1H**, **1G**, and **1S**, the isolated *N,N*-dimethylamino derivatives (**3H**, **3G**, **3S**), and the *N*-methyl dimeric side product (**5G**) were measured via the TEAC assay as shown in Table 4.

All lignin monomers displayed very good antioxidant activity, with **1G** and **1S** significantly outperforming Trolox and Irganox® 3114. In contrast with Irganox, radical scavenging occurred fast as the TEAC values did not change significantly between 5 and 10 minutes. For comparison, **1H**, lacking *ortho*-methoxy moieties, displayed less favorable TEAC values (2.22 after 10 min), indicating a reduced antioxidant activity. For the *N,N*-dimethylamino derivatives (**3H**, **3G**, and **3S**) TEAC values (1.02-1.15 after 10 minutes) were comparable to Trolox and better than Irganox® 3114 (4.19 after 10 minutes) with **3S** outperforming **3H** and **3G**. Overall, these results demonstrate that tertiary amine functionalized lignin monomers could offer a bio-based efficient alternative for their petro-based counterpart.

Table 4. Antioxidant activity as measured by the TEAC assay of lignin monomers and their corresponding tertiary amine obtained via HB with DMA_n.

Compound	TEAC	
	5 min	10 min
Irganox® 3114	6.77	4.19
1H	2.43	2.22
1G	0.82	0.83
1S	0.59	0.59
3H	1.17	1.12
3G	1.15	1.15
3S	1.03	1.02
5G	0.59	0.57

Interestingly, during the HB of **1G** with DMA_n, minor amounts of the dimeric **5G** side product were formed. Although this coupling product was initially considered undesirable, we reasoned that the additional phenolic groups would improve the antioxidant activity. Indeed, the isolated dimer **5G** displays excellent TEAC values, substantially better compared to the monomeric tertiary amines due to the two phenolic groups per molecule. This illustrates that product purification can sometimes be omitted by smart application selection.

CONCLUSION

Efficient upgrading of lignin-derived phenolics, e.g. guaiacols and syringols, to value-added compounds is imperative to the ongoing development of lignocellulose biorefineries. In this contribution, a straightforward hydrogen borrowing methodology was presented to functionalize lignin alcohols into added-value tertiary amines using supported Cu catalysis. Catechol derivatives display strong adhesive interaction with the applied Cu catalyst, thereby impeding catalytic activity. O-demethylation of lignin-derived methoxyphenols, yielding such catechol derivatives, was demonstrated. Using a SiO₂ support with less pronounced acidity/basicity surface properties (*versus* ZrO₂), thereby reducing the detrimental effect of

catechol, formed through O-demethoxylation, proved to be an effective measure to boost the tertiary amine yield. The optimized Cu-SiO₂ hydrogen borrowing protocol was applied to a monomer-enriched RCF lignin oil fraction obtained from spruce wood. Based on the initial content of dihydroconiferyl alcohol, a monomeric tertiary amine yield of 57 mol% was obtained. Looking at the full fraction, semi-quantification by ¹H-¹³C-HSQC NMR gave a 70% overall conversion for all aliphatic γ-POH groups (including mono-, di- and oligomers), which was verified by ³¹P-NMR. A corresponding selectivity of 93% was obtained towards the γ-PNMe₂ functional group. Amination was selective for the end groups, while inter-unit aliphatic alcohols were less reactive for HB and the phenolic hydroxyls remained unaffected. Successful catalytic amination of the lignin dimers was demonstrated and their molecular structures were determined by GC x GC – TOF/MS. The antioxidant capacity of the stable aminated monomers and side products was assessed in an ABTS assay, with the lignin-derived tertiary amines outperforming a commercial phenolic tertiary amine antioxidant. These results prove amination is a precious strategy to further upgrade lignin-derived products to marketable compounds. With dimers and oligomers representing more than 50 wt% of the entire (instead of a partial fractionated) RCF lignin oil, their functionalization and characterization should also be included during lignocellulose upgrading. Although challenging, standard protocols for the detailed quantification of functionalized dimers and oligomers should be developed in the near future. Additionally, this work made clear that heterogeneous catalyst with lignin-derived molecules asks for a careful selection of not only the metal, but also the support. A more detailed assessment of the catalyst surface properties can help to develop even better performing catalyst and will be the focus of future work.

ASSOCIATED CONTENT

Data Availability statement

The data supporting the findings of this study are available from the corresponding author upon reasonable request.

Supporting Information

Detailed information chemicals, materials; Product characterization and purification procedure; ToF SIMS methodology; Classic Irganox® 3114 synthesis; GC x GC chromatograms RFLO's; GC chromatogram catechol; Optimization of hydrogen pressure during HB; Full list of detected species by ToF SIMS analysis; HB results of **1G** for commercial Cu and Ni catalyst. ¹H- and ¹³C-NMR spectral data for the isolated products. Mass spectra and fragmentation pattern obtained after GC x GC analysis for (aminated) dimers.

ACKNOWLEDGEMENT

D.R., B.S. and T.H. acknowledge funding through BIOFACT, a federal research project in Excellence of Science (EoS) call of FWO/FNRS (No.30902231) and the Flemish government for iBOF project Next-BIOREF. T.N. acknowledges the BioApp C3/20/120 – Industrial Research Fund (IOF) KU Leuven for the doctoral fellowship. D.P.D. thanks the Francqui Foundation for the Francqui Research Professor chair. K.V.G. and L.L. acknowledge FWO and innovation program/ERC grant agreement no.818607 (OPTIMA) for funding. LL also acknowledges Cyclops for funding.

REFERENCES

1. Roose, P., Eller, K., Henkes, E., Rossbacher, R. & Höke, H. Amines, Aliphatic. in *Ullmann's Encyclopedia of Industrial Chemistry* 1–55 (Wiley-VCH Verlag GmbH & Co. KGaA, 2015).
2. World Health Organization. World Health Organization Model List of Essential Medicines, 21st List. (2019).
3. Greene, S. A. *Sittig's Handbook of Pesticides and Agricultural Chemicals*. *Sittig's Handbook of Pesticides and Agricultural Chemicals* (Elsevier, 2007).
4. McGrath, N. A., Brichacek, M. & Njardarson, J. T. A Graphical Journey of Innovative Organic Architectures That Have Improved Our Lives. *J. Chem. Educ.* **87**, 1348–1349 (2010).
5. Huang, L., Arndt, M., Gooßen, K., Heydt, H. & Gooßen, L. J. Late Transition Metal-Catalyzed Hydroamination and Hydroamidation. *Chem. Rev.* **115**, 2596–2697 (2015).
6. Cabrero-Antonino, J. R., Adam, R., Papa, V. & Beller, M. Homogeneous and heterogeneous catalytic reduction of amides and related compounds using molecular hydrogen. *Nat. Commun.* **11**, 3893 (2020).
7. Irrgang, T. & Kempe, R. Transition-metal-catalyzed reductive amination employing hydrogen. *Chemical Reviews* **120**, 9583–9674 (2020).
8. Goksu, H., Sert, H., Kilbas, B. & Sen, F. Recent Advances in the Reduction of Nitro Compounds by Heterogenous Catalysts. *Curr. Org. Chem.* **21**, 794–820 (2017).
9. Pelckmans, M., Renders, T., Van de Vyver, S. & Sels, B. F. Bio-based amines through

- sustainable heterogeneous catalysis. *Green Chem.* **19**, 5303–5331 (2017).
10. Froidevaux, V., Negrell, C., Caillol, S., Pascault, J.-P. & Boutevin, B. Biobased Amines: From Synthesis to Polymers; Present and Future. *Chem. Rev.* **116**, 14181–14224 (2016).
 11. Irrgang, T. & Kempe, R. 3d-Metal Catalyzed N- and C-Alkylation Reactions via Borrowing Hydrogen or Hydrogen Autotransfer. *Chemical Reviews* **119**, 2524–2549 (2019).
 12. Bähn, S. *et al.* The Catalytic Amination of Alcohols. *ChemCatChem* **3**, 1853–1864 (2011).
 13. Corma, A., Navas, J. & Sabater, M. J. Advances in One-Pot Synthesis through Borrowing Hydrogen Catalysis. *Chem. Rev.* **118**, 1410–1459 (2018).
 14. Shimizu, K. Heterogeneous catalysis for the direct synthesis of chemicals by borrowing hydrogen methodology. *Catal. Sci. Technol.* **5**, 1412–1427 (2015).
 15. Wu, X., De Bruyn, M. & Barta, K. Primary amines from lignocellulose by direct amination of alcohol intermediates, catalyzed by Raney® Ni. *Catal. Sci. Technol.* **12**, 5908–5916 (2022).
 16. Ruijten, D. *et al.* Hydrogen Borrowing: towards Aliphatic Tertiary Amines from Lignin Model Compounds Using a Supported Copper Catalyst. *ChemSusChem* **15**, (2022).
 17. Elangovan, S. *et al.* From Wood to Tetrahydro-2-benzazepines in Three Waste-Free Steps: Modular Synthesis of Biologically Active Lignin-Derived Scaffolds. *ACS Cent. Sci.* **5**, 1707–1716 (2019).
 18. Shimizu, K. I., Kon, K., Onodera, W., Yamazaki, H. & Kondo, J. N. Heterogeneous Ni

- catalyst for direct synthesis of primary amines from alcohols and ammonia. *ACS Catal.* **3**, 112–117 (2013).
19. Cuypers, T. *et al.* Ni-Catalyzed reductive amination of phenols with ammonia or amines into cyclohexylamines. *Green Chem.* **22**, 1884–1893 (2020).
 20. Van den Bosch, S. *et al.* Tuning the lignin oil OH-content with Ru and Pd catalysts during lignin hydrogenolysis on birch wood. *Chem. Commun.* **51**, 13158–13161 (2015).
 21. Renders, T., Van den Bossche, G., Vangeel, T., Van Aelst, K. & Sels, B. Reductive catalytic fractionation: state of the art of the lignin-first biorefinery. *Current Opinion in Biotechnology* **56**, 193–201 (2019).
 22. Renders, T., Van den Bosch, S., Koelewijn, S.-F., Schutyser, W. & Sels, B. F. Lignin-first biomass fractionation: the advent of active stabilisation strategies. *Energy Environ. Sci.* **10**, 1551–1557 (2017).
 23. Van Aelst, K. *et al.* Reductive catalytic fractionation of pine wood: elucidating and quantifying the molecular structures in the lignin oil. *Chem. Sci.* **11**, 11498–11508 (2020).
 24. Dao Thi, H. *et al.* Identification and quantification of lignin monomers and oligomers from reductive catalytic fractionation of pine wood with GC × GC – FID/MS. *Green Chem.* **24**, 191–206 (2022).
 25. Lancefield, C. S., Wienk, H. L. J., Boelens, R., Weckhuysen, B. M. & Bruijninx, P. C. A. Identification of a diagnostic structural motif reveals a new reaction intermediate and condensation pathway in kraft lignin formation. *Chem. Sci.* **9**, 6348–6360 (2018).
 26. Lu, X., Gu, X. & Shi, Y. A review on lignin antioxidants: Their sources, isolations,

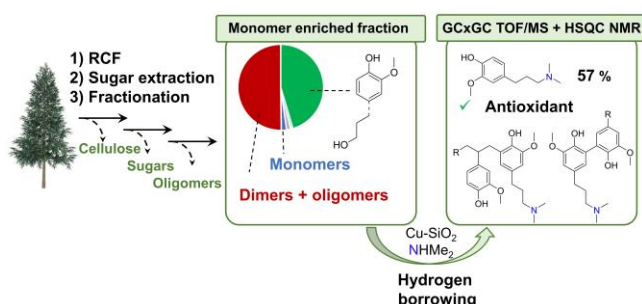
- antioxidant activities and various applications. *Int. J. Biol. Macromol.* **210**, 716–741 (2022).
27. C., L. R., Vinqvist, B. & Vinqvist, M. R. Phenols as antioxidants. in *The chemistry of Phenols* (ed. Rappoport, Z.) 840–902 (2003).
 28. Li, C., Sun, P., Yu, H., Zhang, N. & Wang, J. Scavenging ability of dendritic PAMAM bridged hindered phenolic antioxidants towards DPPH[•] and ROO[•] free radicals. *RSC Adv.* **7**, 1869–1876 (2017).
 29. Dyubchenko, O. I., Nikulina, V. V., Terakh, E. I., Prosenko, A. E. & Grigor'ev, I. A. Synthesis and Antioxidative Activity of N, N-Dialkyl-ω-[4-hydroxy(methoxy)aryl]alkylamines and Their N-Oxides. *Russ. J. Appl. Chem.* **78**, 781–786 (2005).
 30. Rowland, R. G., Dong, J. & Migdal, C. A. Antioxidants. in *Lubricant Additives* 3–36 (CRC Press, 2017).
 31. Buvik, V., Vevelstad, S. J., Brakstad, O. G. & Knuutila, H. K. Stability of Structurally Varied Aqueous Amines for CO₂ Capture. *Ind. Eng. Chem. Res.* **60**, 5627–5638 (2021).
 32. Guo, J. & Chongxin, Z. Patent WO2020238188: Process for synthesizing antioxidant 3114. (2020).
 33. Gu, Q. & Qiu, X. Patent CN1101909: Atmospheric solvent process for synthesizing antioxidant di-tert-butyl-hydroxy-benzyl isocyanurate. (1993).
 34. BASF. Irganox 3114 - Technical Datasheet. (2022). Available at: <https://polymer-additives.specialchem.com/product/a-basf-irganox-3114>.

35. Roose, P. Methylamines. in *Ullmann's Encyclopedia of Industrial Chemistry* 1–10 (Wiley-VCH Verlag GmbH & Co. KGaA, 2015).
36. Ilyasov, I. R., Beloborodov, V. L., Selivanova, I. A. & Terekhov, R. P. ABTS/PP Decolorization Assay of Antioxidant Capacity Reaction Pathways. *Int. J. Mol. Sci.* **21**, 1131 (2020).
37. Re, R. *et al.* Antioxidant activity applying an improved ABTS radical cation decolorization assay. *Free Radic. Biol. Med.* **26**, 1231–1237 (1999).
38. Sudarsanam, P. *et al.* Towards Lignin-Derived Chemicals Using Atom-Efficient Catalytic Routes. *Trends Chem.* **2**, 898–913 (2020).
39. Fujisawa, S., Kadoma, Y. & Yokoe, I. Radical-scavenging activity of butylated hydroxytoluene (BHT) and its metabolites. *Chem. Phys. Lipids* **130**, 189–195 (2004).
40. Saiz-Poseu, J., Mancebo-Aracil, J., Nador, F., Busqué, F. & Ruiz-Molina, D. The Chemistry behind Catechol-Based Adhesion. *Angew. Chemie Int. Ed.* **58**, 696–714 (2019).
41. Wu, X. *et al.* Lignin-First Monomers to Catechol: Rational Cleavage of C–O and C–C Bonds over Zeolites. *ChemSusChem* **15**, (2022).
42. Popov, A. *et al.* Bio-oils Hydrodeoxygenation: Adsorption of Phenolic Molecules on Oxidic Catalyst Supports. *J. Phys. Chem. C* **114**, 15661–15670 (2010).
43. De Clercq, R. *et al.* Titania-Silica Catalysts for Lactide Production from Renewable Alkyl Lactates: Structure–Activity Relations. *ACS Catal.* **8**, 8130–8139 (2018).
44. Grams, J. *New trends and potentialities of ToF-SIMS in surface studies.* (Nova Publisers, 2007).

45. Ruppert, A. M., Grams, J., Matras-Michalska, J., Chelwicka, M. & Przybysz, P. ToF-SIMS study of the surface of catalysts used in biomass valorization. *Surf. Interface Anal.* **46**, 726–730 (2014).
46. Weng, L.-T. Advances in the surface characterization of heterogeneous catalysts using ToF-SIMS. *Appl. Catal. A Gen.* **474**, 203–210 (2014).
47. Xu, W., Huang, Z., Ji, X. & Lumb, J.-P. Catalytic Aerobic Cross-Dehydrogenative Coupling of Phenols and Catechols. *ACS Catal.* **9**, 3800–3810 (2019).
48. Ibáñez, J., Araque-Marin, M., Paul, S. & Pera-Titus, M. Direct amination of 1-octanol with NH₃ over Ag-Co/Al₂O₃: Promoting effect of the H₂ pressure on the reaction rate. *Chem. Eng. J.* **358**, 1620–1630 (2019).
49. Popov, A. *et al.* Bio-oil hydrodeoxygenation: Adsorption of phenolic compounds on sulfided (Co)Mo catalysts. *J. Catal.* **297**, 176–186 (2013).
50. Dang, Z., Anderson, B. G., Amenomiya, Y. & Morrow, B. A. Silica-Supported Zirconia. 1. Characterization by Infrared Spectroscopy, Temperature-Programmed Desorption, and X-ray Diffraction. *J. Phys. Chem.* **99**, 14437–14443 (1995).
51. Zhang, Y., Pan, L., Gao, C., Wang, Y. & Zhao, Y. Preparation of ZrO₂–SiO₂ mixed oxide by combination of sol–gel and alcohol-aqueous heating method and its application in tetrahydrofuran polymerization. *J. Sol-Gel Sci. Technol.* **56**, 27–32 (2010).
52. Zhu, Y. *et al.* Highly selective synthesis of ethylene glycol and ethanol via hydrogenation of dimethyl oxalate on Cu catalysts: Influence of support. *Appl. Catal. A Gen.* **468**, 296–304 (2013).
53. Liao, Y. *et al.* A sustainable wood biorefinery for low-carbon footprint chemicals

- production. *Science* (80-.). **367**, 1385–1390 (2020).
54. Jedrzejczyk, M. A. *et al.* Lignin-Based Additives for Improved Thermo-Oxidative Stability of Biolubricants. *ACS Sustain. Chem. Eng.* **9**, 12548–12559 (2021).
 55. Lane, J. Clearing the Confusion: GPC, SEC, GFC – What , When, Why, and How? (2017). Available at:
https://www.agilent.com/cs/library/eseminars/public/Clearing_the_Confusion_Webinar.pdf.
 56. Abu-Omar, M. M. *et al.* Guidelines for performing lignin-first biorefining. *Energy Environ. Sci.* **14**, 262–292 (2021).
 57. Suota, M. J. *et al.* Lignin functionalization strategies and the potential applications of its derivatives – A Review. *BioResources* **16**, 6471–6511 (2021).
 58. Sun, Z., Fridrich, B., de Santi, A., Elangovan, S. & Barta, K. Bright Side of Lignin Depolymerization: Toward New Platform Chemicals. *Chem. Rev.* **118**, 614–678 (2018).
 59. Jia, Y., He, Y. & Lu, F. The structure-antioxidant activity relationship of dehydrodiferulates. *Food Chem.* **269**, 480–485 (2018).

For Table of Contents Use Only



SYNOPSIS

RCF lignin monomers and dimers are effectively converted to tertiary amines with antioxidant activity via a Cu-catalyzed hydrogen borrowing strategy.